Dimensional Analysis of the Earthquake-induced Pounding between Adjacent Structures

Elias Dimitrakopoulos,[1] Nicos Makris,[2] and Andreas J. Kappos[3]

Abstract

In this paper the dynamic response of two and three pounding oscillators subjected to pulse type excitations is revisited with dimensional analysis. Using Buckingham's Π-theorem the number of variables that govern the response of the system is reduced by three. When the response is presented in the dimensionless Π-terms remarkable order emerges. It is shown that regardless of the acceleration level and duration of the pulse all response spectra become self-similar and follow a single master curve. This is true despite the realization of finite duration contacts with increasing durations as the excitation level increases. All physically realizable contacts (impacts, continuous contacts, and detachments) are captured via a linear complementarity approach. The study confirms the existence of three spectral regions. The response of the most flexible among the two oscillators amplifies in the low range of the frequency spectrum (flexible structures); whereas, the response of the most stiff among the two oscillators amplifies at the upper range of the frequency spectrum (stiff structures). Most importantly, the study shows that pounding structures such as colliding buildings or interacting bridge segments, may be most vulnerable for excitations with frequencies very different from their natural eigenfrequencies. Finally, by applying the concept of *intermediate asymptotics*, the study unveils that the dimensionless response of two pounding oscillators follows a scaling law with respect to the mass ratio, or in mathematical terms, that the response exhibits an incomplete self-similarity or self-similarity of the second kind with respect to the mass ratio.

Keywords: Pounding, Unilateral Contact, Dimensional Analysis, Earthquake Engineering

[1]Doctoral Candidate, Dept. of Civil Engineering, Aristotle University of Thessaloniki, Greece, GR 54124
[2]Professor, Dept. of Civil Engineering, University of Patras, Greece, GR 26500
[3]Professor, Dept. of Civil Engineering, Aristotle University of Thessaloniki, Greece, GR 54124

INTRODUCTION

This paper belongs to a wider study on the problem of pounding between adjacent structures due to earthquake shaking, which is revisited herein with the help of formal dimensional analysis [1-3]. The motivation for this study originates partly from the large number of parameters that govern the response of pounding oscillators and partly from several conflicting conclusions published in the literature.

Analytical studies on the response of a linear single-degree of freedom oscillator with one-sided contact have been presented, among others, by Davis [4]. The work of Davis [4] for harmonic excitation was extended by Chau & Wei [5], who studied the response of two colliding SDOF oscillators with elastic and inelastic impact. They observed that the '*impact-velocity*' spectrum is not sensitive to the size of the gap between the two oscillators and they concluded that impact amplified the response of the stiffer oscillator while suppressing the response of the more flexible oscillator and that the gap needed to avoid impact is the maximum when the excitation frequency approaches the natural frequency of the flexible oscillator.

The impact between adjacent buildings due to earthquake shaking has often been recorded as one of the causes of structural damage (Anagnostopoulos [6], [7], Anagnostopoulos & Spiliopoulos [8], Penelis & Kappos [9] and references reported therein). The studies of Anagnostopoulos and his coworkers concluded that pounding can amplify or reduce the earthquake response of a building depending upon its period and mass in relation to the period and mass of the buildings next to it, and that when the masses of the two interacting buildings are similar the response of the stiffer building will amplify, a result that is in agreement with the conclusions of Chau & Wei [5].

Maragakis [10] studied the rigid body motions of bridge decks, triggered by the impact between the deck and the abutments. Using a simplified stick model, he focused on the impact-based planar rigid body rotations of skew bridges. Liolios [11] addressed the problem of building pounding by adopting the formulation of unilateral contacts initially developed by Panagiotopoulos [12] – a formulation which, in essence, is also adopted in this paper for modeling impact and contact.

The impact of many SDOF oscillators in a row has been studied by Anagnostopoulos [6] and Athanassiadou et al. [13] with emphasis on buildings, and by Jankowski et al. [14] with emphasis on multi-span bridges. Further studies on the impact of bridge segments have been presented by DesRoches & Muthukumar [15] who examined the impact response of elastic and inelastic oscillators including the event of adjacent structures restrained with cables. That study concludes that among the dominant parameters which govern the pounding response are the stiffness ratio of the neighboring oscillators together with the ratio of the natural period of one of the oscillators and the dominant period of the excitation. A further conclusion of the DesRoches & Muthukumar [15] work is that when the natural frequency and the excitation frequency are separated the one-sided impact is accentuated, whereas, impact suppresses the response of the oscillators at resonance. At about the same time an analogous study was conducted in Japan by Ruangrassame & Kawashima [16] who proposed the so-called '*relative displacement response spectrum with pounding effect'*. Contrary to the work of DesRoches & Muthukumar the work of Ruangrassame & Kawashima concluded that in addition to the stiffness ratio and the period ratio, the mass ratio of the two oscillators governs appreciably the response.

Part of the motivation of the work reported herein is the need to resolve the aforementioned conflicting conclusions together with the need to uncover the fundamental physical similarities that describe the pounding oscillators. This is achieved by implementing the theory of dimensional analysis which offers a lucid interpretation of the response. This paper concentrates on bringing forward and explaining the physical similarities of the earthquake induced pounding between adjacent structures. In particular, the present analysis concerns structures which can be adequately modeled as single degree-of-freedom (SDOF) elastic oscillators. For instance, adjacent segments of segmented bridges, which due to their strong columns (the modern practice in the design of segmented bridges) are often expected to remain elastic even for motions which are much more intense that the design earthquake. While the elastic SDOF model is an elementary model, the pounding response of adjacent SDOF oscillators is, as this paper shows, already complicated. Moreover, with the selection of the same models that were used in references [4, 5, and 6] the study illustrates directly the merits of adopting formal dimensional analysis and helps in resolving the aforementioned conflicting conclusions. The dimensionless parameters that govern the response of the elastoplastic pounding oscillator, which is

a more representative model for seismically isolated structures, are also presented herein.

The application of the proposed method hinges upon the existence of a distinct time scale and a length scale that characterize the most energetic component of ground shaking. Such time and length scales emerge naturally from the distinguishable pulses which dominate a wide class of strong earthquake records; they are directly related with the rise time and slip velocity of faulting and can be formally extracted with validated mathematical models published in the literature.

The minimum number of input parameters of such models is two and they have an unambiguous physical meaning. These are either their acceleration amplitude, α_p, and duration, T_p or the velocity amplitude, v_p, and duration, T_p. Figure 1 shows the time histories of the Rinaldi station record, from the 1994 Northridge earthquake, the OTE record from the 1995 Aegion earthquake, and the Bucharest record of the 1977 Vrancea earthquake, are also shown. In all three records the pulse duration, T_p, and the pulse acceleration, α_p, are shown. The current established methodologies for estimating the pulse characteristics of a wide class of records are of unique value, since the product $\alpha_p T_p^2 \sim L_e$ is a characteristic length scale of the ground excitation and is a measure of the persistence of the most energetic pulse to impose deformation demands, see for instance Dimitrakopoulos et al. [17] for the pounding oscillator and Makris & Black [18-20], Makris & Psychogios [21] for yielding oscillators.

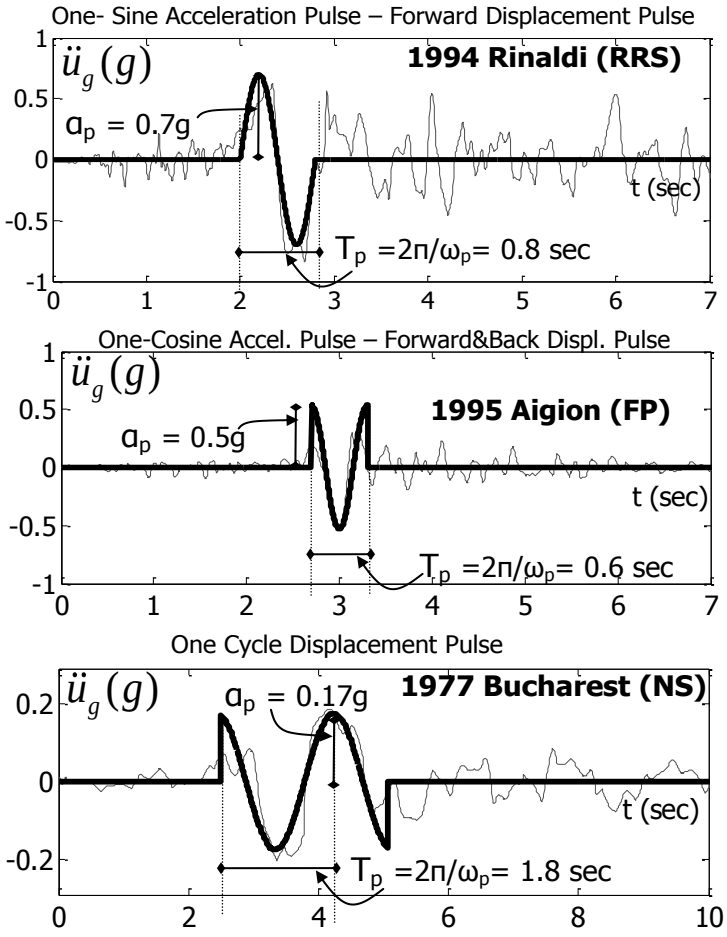

Figure 1 Earthquake records with distinguishable acceleration pulse.

MATHEMATICAL FORMULATIONS ON IMPACT AND CONTACT

All physically feasible unilateral contact configurations (impacts, continuous contacts, and detachments) are mathematically treated as inequality problems; namely Linear Complementarity Problems (LCP) following the non-smooth approach proposed by Pfeiffer & Glocker [22]. In the classical form, a LCP is a system of linear equations: $\mathbf{y} = \mathbf{A}\mathbf{x} + \mathbf{b}$, with matrices **A** and **b** known, and ***y*** and ***x*** the unknown vectors under determination, for which the following additional complementarity conditions hold: $\mathbf{y} \geq 0, \ \mathbf{x} \geq 0, \ \mathbf{y}^T\mathbf{x} = 0$ [22, 23].

According to Leine et al. [23], two similar LCPs are formulated at the velocity level in order to capture the velocity jumps associated with the two impact phases (compression and expansion) and one additional LCP is formulated at the acceleration level for the treatment of continuous contacts and detachment. In the following, the aforementioned LCPs are presented in a simplified version, since in the present study, contact is assumed to be frictionless and centric.

Continuous Contact and Detachment: Assuming the impenetrability constraint of the contact surface holds, then the relative distance in the normal (to the contact surface) direction of a contact, $\mathbf{g}_\mathbf{N}$, must always satisfy the inequality constraint: $\mathbf{g}_\mathbf{N} \geq 0$. Every time, the normal distance vanishes, $\mathbf{g}_\mathbf{N}(t) = 0$, contact takes place. With respect to the normal direction of a contact, there are two types of contacts: the instantaneous (impacts) and the continuous (finite duration) contacts which appear when additionally the relative velocity of the contacting bodies, $\dot{\mathbf{g}}_\mathbf{N}(t) = 0$, vanishes. This can be either due to totally plastic impact, or successive inelastic impacts. A continuous contact results in a contact force, λ, which can be calculated as a Lagrange multiplier that must satisfy the constraint: $\lambda \geq 0$ due to the unilateral character of a contact, the pertinent LCP is formulated on the acceleration level as in [23]:

$$\ddot{\mathbf{g}}_\mathbf{N} = \mathbf{W}^T\mathbf{M}^{-1}\mathbf{h} + \mathbf{W}^T\mathbf{M}^{-1}\mathbf{W}\,\boldsymbol{\lambda}, \ \ \ddot{\mathbf{g}}_\mathbf{N} \geq 0, \ \boldsymbol{\lambda} \geq 0, \ \ddot{\mathbf{g}}_\mathbf{N} \cdot \boldsymbol{\lambda} = 0 \qquad \textbf{(1)}$$

where: ***M*** is the mass matrix, ***W*** is the direction vector of the constraint contact force, ***λ***, which can be considered as a Lagrange multiplier and ***h*** is the vector of the non-impulsive forces.

Impact: Compression - Expansion Phases: At the end of the compression phase of impact, the relative velocity, $\dot{g}_{NC}$, and the impulse, $\boldsymbol{\Lambda}_{NC}$, in the normal direction of the contact, form a LCP which can be written as:

$$\dot{\mathbf{g}}_{NC} = \mathbf{W}^T\mathbf{M}^{-1}\mathbf{W}\,\boldsymbol{\Lambda}_{NC} + \dot{\mathbf{g}}_{NA}, \ \ \dot{\mathbf{g}}_{NC} \geq 0, \ \boldsymbol{\Lambda}_{NC} \geq 0, \ \dot{\mathbf{g}}_{NC} \cdot \boldsymbol{\Lambda}_{NC} = 0 \qquad \textbf{(2)}$$

where sub-index *N* stands for the normal direction of contact, sub-indices *C, E* and *A* stand for compression, expansion (see Eq. 3) phase and the time instant contact begins, respectively, ***Λ***, stands for impulse of contact.

Similarly, the relative velocity at the end of the expansion phase, $\dot{\mathbf{g}}_{NE}$, forms a LCP with the impulse, $\boldsymbol{\Lambda}_{NP} = \boldsymbol{\Lambda}_{NE} - \boldsymbol{\varepsilon}_N\boldsymbol{\Lambda}_{NC}$, which can be written as:

$$\dot{\mathbf{g}}_{NE} = \left(\mathbf{W}^T\mathbf{M}^{-1}\mathbf{W}\right)\boldsymbol{\Lambda}_{NP} + \mathbf{W}^T\mathbf{M}^{-1}\mathbf{W}\boldsymbol{\varepsilon}_N\boldsymbol{\Lambda}_{NC} + \dot{\mathbf{g}}_{NC}, \ \ \dot{\mathbf{g}}_{NE} \geq 0, \ \boldsymbol{\Lambda}_{NE} \geq 0, \ \dot{\mathbf{g}}_{NE} \cdot \boldsymbol{\Lambda}_{NE} = 0 \qquad \textbf{(3)}$$

The contact law utilized in the present study is that of Poisson's, according to which the coefficient of restitution, ε_N, is the impulse ratio of the approach and expansion phases. It is reminded that Newton's coefficient of restitution is taken as the ratio of the (relative) contact velocities after, $\dot{\mathbf{g}}_{NE}$, and before, $\dot{\mathbf{g}}_{NA}$, impact: $\dot{\mathbf{g}}_{NE} = -\boldsymbol{\varepsilon}_N\dot{\mathbf{g}}_{NA}$. However, as shown in [22], Poisson's model yields more realistic results than Newton's, for the more complex case of multi-contact configurations.

ELASTIC OSCILLATORS WITH UNILATERAL CONTACT SUBJECTED TO BASE EXCITATION

Two configurations, of two and three elastic SDOF pounding oscillators in a row (Figure 2), are considered in the present study. The equation of motion, taking into account contact phenomena, of the mechanical systems of Figure 2 can be written as:

$$\mathbf{M\ddot{u} + C\dot{u} + Ku - W \cdot \lambda = -M d}\ddot{u}_g(t) \quad \textbf{(4)}$$

where $\boldsymbol{u}$ is the relative, to the ground, response displacement vector, u_g is the ground displacement, $\boldsymbol{M}$, $\boldsymbol{C}$ and $\boldsymbol{K}$, are the mass, damping, and stiffness matrices, respectively, $\boldsymbol{W}$ is the direction vector of the constraint contact force $\boldsymbol{\lambda}$ and $\boldsymbol{d}$ is the unit vector. For the most general case of the three oscillators (Figure 2) these matrices specify to:

$\mathbf{u}^{\mathbf{T}} = [u_1 \quad u_0 \quad u_2]$, $\mathbf{M} = diag\{m_1, m_0, m_2\}$, $\mathbf{C} = diag\{c_1, c_0, c_2\}$, $\mathbf{K} = diag\{k_1, k_0, k_2\}$, and $\mathbf{d}^{\mathbf{T}} = [1 \quad 1 \quad 1]$. For clarity and convenience, the oscillator whose response is discussed in detail in each configuration, is in all cases denoted with subscript '0'.

There are two potential contact points among three adjacent oscillators in a row: contact '1' between the first and the second oscillator in the row and contact '2' between the second and the third (Figure 2 bottom). The normal distances of the two contacts, are respectively: $g_{N1}(t) = \delta - u_1(t) + u_0(t)$, $g_{N2}(t) = \delta - u_0(t) + u_2(t)$ and thus the pertinent direction vectors become: $\mathbf{W}_1^T = [-1 \quad 1 \quad 0]$ and $\mathbf{W}_2^T = [0 \quad -1 \quad 1]$.

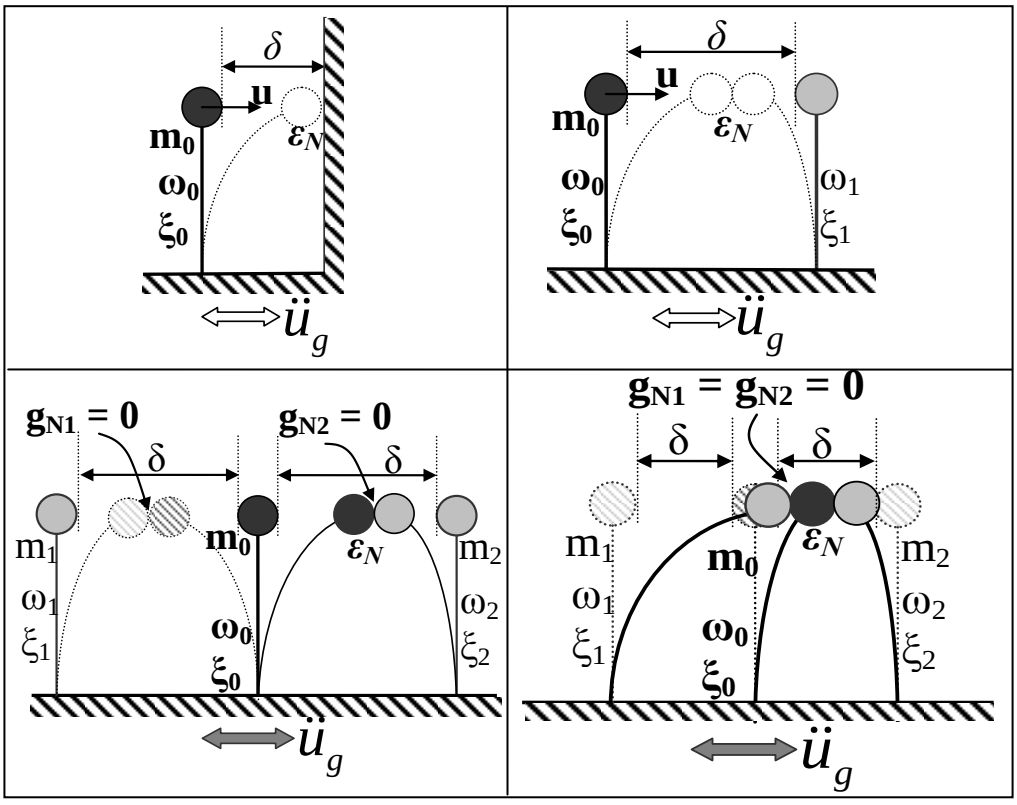

Figure 2 Configurations of pounding structures subjected to pulse-type ground motions (top). Simple (bottom left) and double (bottom right) unilateral contact configuration of three oscillators.

Referring to unilateral contact, which herein is assumed as centric and frictionless, a fundamental difference among the two and the three pounding oscillators' configuration should be noted. In the three pounding oscillators system, there is the likelihood of a multiple (double) contact, which occurs when both normal distances of the contacts vanish ($g_{N1} = g_{N2} = 0$, Figure 2 bottom). Furthermore, these two simultaneous contacts may be of a different type (impact / continuous contact).

A refined approach to account for these complexities is that of Pfeiffer & Glocker [22], in the form presented more recently by Leine et al. [23], see also Dimitrakopoulos et al. [17].

IMPLEMENTATION OF DIMENSIONAL ANALYSIS

The parameters governing the response of three pounding oscillators subjected to ground excitation (Figure 2) are: a response quantity of interest e.g. the maximum response displacement of the centric oscillator u_{max}, the angular frequency, mass, and damping ratio of the associated oscillators: ω_0, m_0, ξ_0, ω_1, m_1, ξ_1, and ω_2, m_2, ξ_2, respectively, the acceleration amplitude and the angular frequency of the pulse, α_p and $\omega_p = 2\pi/T_p$ (Figure 1), the initial distance between the oscillators "gap", δ, and the coefficient of restitution, ε_N . Thus the response function can be written as:

$$u_{\max} = f(\omega_0, \omega_1, \omega_2, m_0, m_1, m_2, \delta, a_p, \omega_p, \varepsilon_N, \xi_0, \xi_1, \xi_2) \quad \textbf{(5)}$$

This results in a group of 14 characteristic variables. In order to reduce the number of parameters under investigation, it is assumed that viscous damping in all oscillators is the same ($\xi = 5\%$). This leaves 11 variables which involve 3 reference dimensions, those of length [L], time [T] and mass [M]. According to Buckingham's "Π" theorem the number of independent dimensionless Π-products is now: (11 variables) – (3 reference dimensions) = 8 Π-terms.

Herein, the characteristics of the pulse excitation, α_p and $\omega_p = 2\pi/T_p$, and the properties of the reference-oscillator, ω_0, m_0 and ξ_0 are selected as repeating variables, since we desire to normalize the non-linear response including contact, to the energetic length scale of the excitation, $L_e = \alpha_p/\omega_p^2$. Accordingly, Eq.(5) reduces to:

$$\frac{u_{\max}\omega_p^2}{a_p} = \phi\left(\frac{\omega_0}{\omega_p}, \frac{\delta\omega_p^2}{a_p}, \varepsilon_N, \frac{\omega_0}{\omega_1}, \frac{m_0}{m_1}, \frac{\omega_0}{\omega_2}, \frac{m_0}{m_2}\right) \quad \textbf{(6)}$$

or

$$\Pi_1 = \phi(\Pi_2, \Pi_3, \Pi_4, \Pi_5, \Pi_6, \Pi_7, \Pi_8) \Rightarrow \quad \textbf{(7)}$$

with:

$$\Pi_1 = \frac{u_{\max}\omega_p^2}{a_p}, \Pi_2 = \frac{\omega_0}{\omega_p}, \Pi_3 = \frac{\delta\omega_p^2}{a_p}, \Pi_4 = \varepsilon_N, \Pi_5 = \frac{\omega_0}{\omega_1}, \Pi_6 = \frac{m_0}{m_1}, \Pi_7 = \frac{\omega_0}{\omega_2}, \Pi_8 = \frac{m_0}{m_2} \quad \textbf{(8)}$$

Note that, from these 8 Π-products of Eq.7, only the six first, Π_1 to Π_6 (Eq. 8), are needed in order to describe the response of the two pounding oscillators shown in Figure 2, as well as, the response of a symmetric configuration of three pounding oscillators wherein the outer oscillators are identical, $\omega_1 = \omega_2$, $m_1 = m_2$, which will be of interest in a later section. Also, observe that, in contrast to the single pounding oscillator case [17], masses cannot be eliminated from equation (6) unless $m_0 = m_1 = m_2 = m$, which is a very special case.

The dimensionless product, $\Pi_1 = u_{max}\omega_p^2/a_p$ which is the dependent variable, is the maximum response displacement normalized to the persistency of the pulse L_e =

a_p/ω_p^2. $\Pi_2 = \omega_0/\omega_p$, is the natural frequency of the examined oscillator divided by the frequency of the pulse and the dimensionless $\Pi_4 = \varepsilon_N$ term is the coefficient of restitution, which expresses the inelasticity of impact; with $\varepsilon_N = 1$ corresponding to a perfectly elastic, and $\varepsilon_N = 0$ to a perfectly plastic, impact.

The additional dimensionless products which appear when examining a system of more than one SDOF pounding oscillator, are the frequency ratios and the mass ratios of the involved oscillators, e.g. $\Pi_5 = \omega_0/\omega_1 = T_1/T_0$ and $\Pi_6 = m_0/m_1$. In later sections of the present paper, the role of these terms is investigated in depth.

The product $\Pi_3 = \delta\omega_p^2/a_p$ is a novel proposition which suggests that the size of the gap "δ" can be scaled to the length scale of the excitation (a_p/ω_p^2 [m]) which is a measure of the persistence of the energetic pulse (Makris & Black, [18-20]). The most decisive feature of the Π_3-term approach is that it brings forward the property of self-similarity for configurations with multiple SDOF oscillators. For instance, Figure 3 shows the response of the central oscillator in an asymmetric configuration of three pounding oscillators, subjected to one-cycle displacement pulses of different intensity. Figure 3 illustrates the self-similar response spectra for a constant dimensionless gap, Π_3, and different excitation intensities (Figure 3 left column), which collapse to a single-master curve, when expressed in the dimensionless Π- terms (right column). Response curves for the no-contact case are also included in Figure 3 for better interpretation of self-similarity, since it is a well known property of linear elastic response.

Note that, had the gap size, δ, been scaled to the relative displacement of the hinge when contact of the adjacent structures does not occur, i.e. the more common way of $\chi = \delta/u_{NoPounding}$ ratio, the two contacts would yield different dimensionless gap values, χ_1 and χ_2 respectively. On the contrary, using the dimensionless Π_3 product, a single value is needed to describe all contact points with the same gap size, δ; hence a superior presentation of the response is achieved.

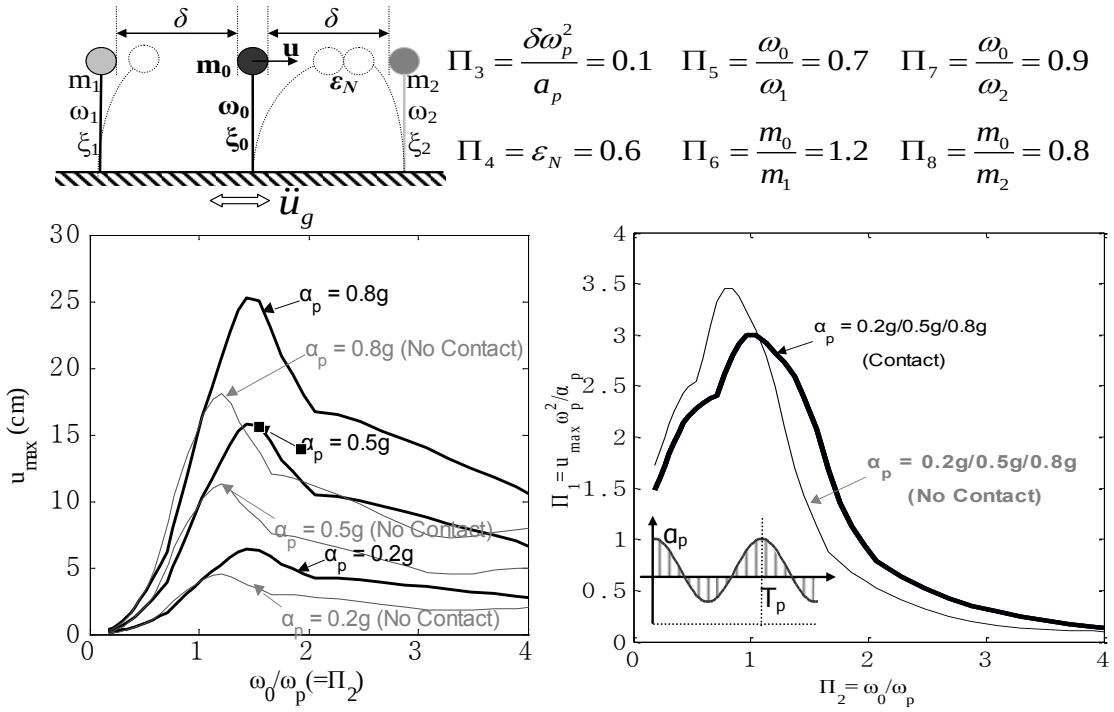

Figure 3 The self-similar response spectra for different excitation intensities and a given dimensionless gap value, Π_3, (left) collapse to a single curve when expressed in the proposed dimensionless Π – terms (right). (heavy lines= contact, light lines = No contact).

Following the same reasoning, the concept of dimensional analysis can be applied to more general yielding systems. For instance, if uy is the yield displacement and Q/m the characteristic strength of an elastoplastic oscillator pounding against a rigid barrier (Figure 2 top left), then its response function can be written as:

$$u_{\max} = f(u_y, Q/m, \delta, \varepsilon_N, a_p, \omega_p) \Rightarrow \frac{u_{\max}\omega_p^2}{a_p} = \phi\left(\frac{Q}{ma_p}, \frac{\delta\omega_p^2}{a_p}, \varepsilon_N, \frac{u_y\omega_p^2}{a_p}\right) \qquad (9)$$

The dimensional response analysis of the elastoplastic and bilinear pounding oscillators will be the subject of a future study.

THE INFLUENCE OF THE OSCILLATORS' STIFFNESS RATIO ON THE RESPONSE

The influence of the frequency ratio, $\Pi_5 = \omega_0/\omega_1 = T_1/T_0$, of the two pounding oscillators is first examined, considering the special case of equal masses, $\Pi_6 = m_0/m_1 = 1$, (Figure 4 and Figure 5). Since the mass is considered the same for the two structures, it follows that the difference in frequencies is caused by different stiffness, thus:

$$if \quad \Pi_6 = \frac{m_0}{m_1} = 1 \Rightarrow \Pi_5 = \frac{\omega_0}{\omega_1} = \frac{T_1}{T_0} = \sqrt{\frac{k_0}{k_1}} \qquad \textbf{(10)}$$

Figure 4 and Figure 5 show the response spectra of the oscillator with subscript '0' for the case of equal masses, $\Pi_6 = m_0/m_1 = 1$, and a wide rage of frequency ratios of the two oscillators, $\Pi_5 = \omega_0/\omega_1$, from 0.1 to 10. In all cases shown, the gap size is scaled to the energetic length of the pulse and is identical, namely: $\Pi_3 = \delta\omega_p^2/a_p = 0.5$. As the frequency ratio, dimensionless Π_5 product, increases from 0.1 to 10, the oscillator under consideration varies from the most flexible (left column) to the most stiff (right column) of the system, thus revealing the influence of the stiffness ratio in all cases.

The two SDOF pounding oscillators configuration is not symmetric, hence there is a distinction whether the pulse is of normal or reverse directivity (Figure 4 and Figure 5), with respect to the oscillator under examination, denoted with subscript zero. In both Figures (4 and 5) the left column refers to the results of the most flexible oscillator, $\Pi_5 = \omega_0/\omega_1 < 1$, and the right column to the results of the most stiff, $\Pi_5 = \omega_0/\omega_1 > 1$, while the first row corresponds to a forward displacement (one sine acceleration) excitation pulse and the second to a forward and back displacement (one cosine acceleration) pulse. Again, response without contact, denoted with a light line, is included for comparison.

It is recalled that for $\Pi_5 = \omega_0/\omega_1$ the two structures are oscillating in phase, hence maintaining their relative distance, and since no phase difference or spatial variation is considered for the ground excitation, no contact takes place. So, as the frequency ratio of the two oscillators approaches unity ($\Pi_5 \rightarrow 1$), the behavior of the oscillator under consideration, converges to the response without contact.

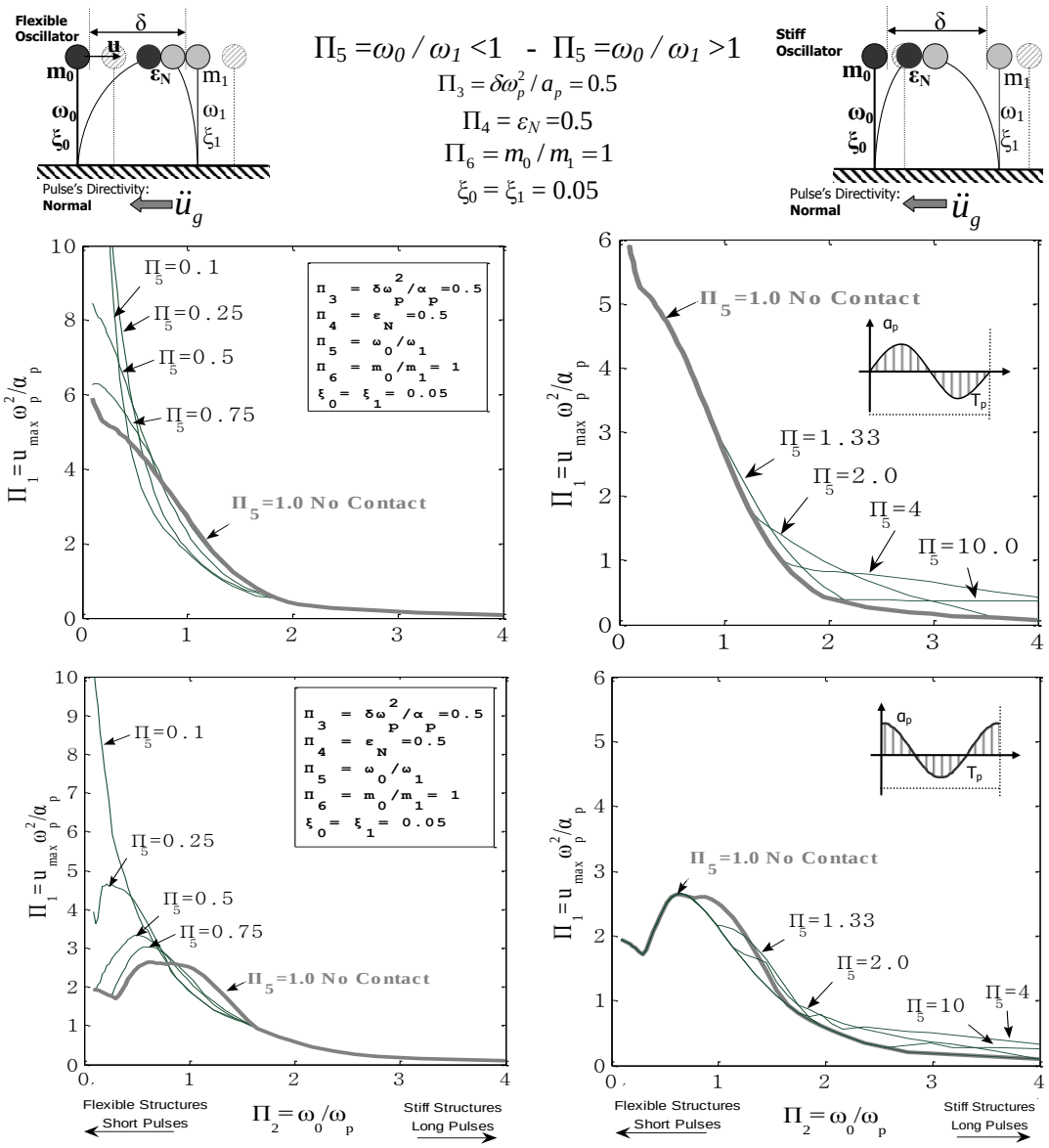

Figure 4. Self-similar response spectra (master curves) for the mechanical system of two SDOF oscillators subjected to a one sine (top) and one cosine (bottom) acceleration pulse of normal directivity. Left column corresponds to most flexible - right column to most stiff among the two oscillators, and results are shown for several stiffness ratios.

Furthermore, Figure 4 and Figure 5 disclose that due to unilateral contact, the response of the most flexible, as well as of the most stiff, among the two oscillators is both amplified and deamplified, depending on the corresponding range of the frequency spectrum ($\Pi_2 = \omega_0/\omega_p$ values). Observe in Figure 4 and Figure 5 that the maxima of the flexible oscillator occur at the resonant frequency of the other, more stiff, oscillator. For instance, if the frequency ratio of the two oscillators is $\Pi_5 = \omega_0 / \omega_1 = 0.5$, the flexible oscillator presents a maximum displacement (see Figure 4 and Figure 5) for $\Pi_2 = \omega_0 / \omega_p = 0.5$ which corresponds to the resonant frequency of the stiffer oscillator ($\omega_p = \omega_1 = 1.0$, $\Pi_2 = \Pi_5$). A similar trend can be identified for the stiffer oscillator, since its response displacement (in dimensionless terms) is also amplified at the resonant frequency of the more flexible oscillator, even though it preserves its global maximum near its original resonant frequency. Figure 6 presents

two time history shows where the response of both the flexible and the stiff oscillator are accentuated for different excitation frequencies due to contact.

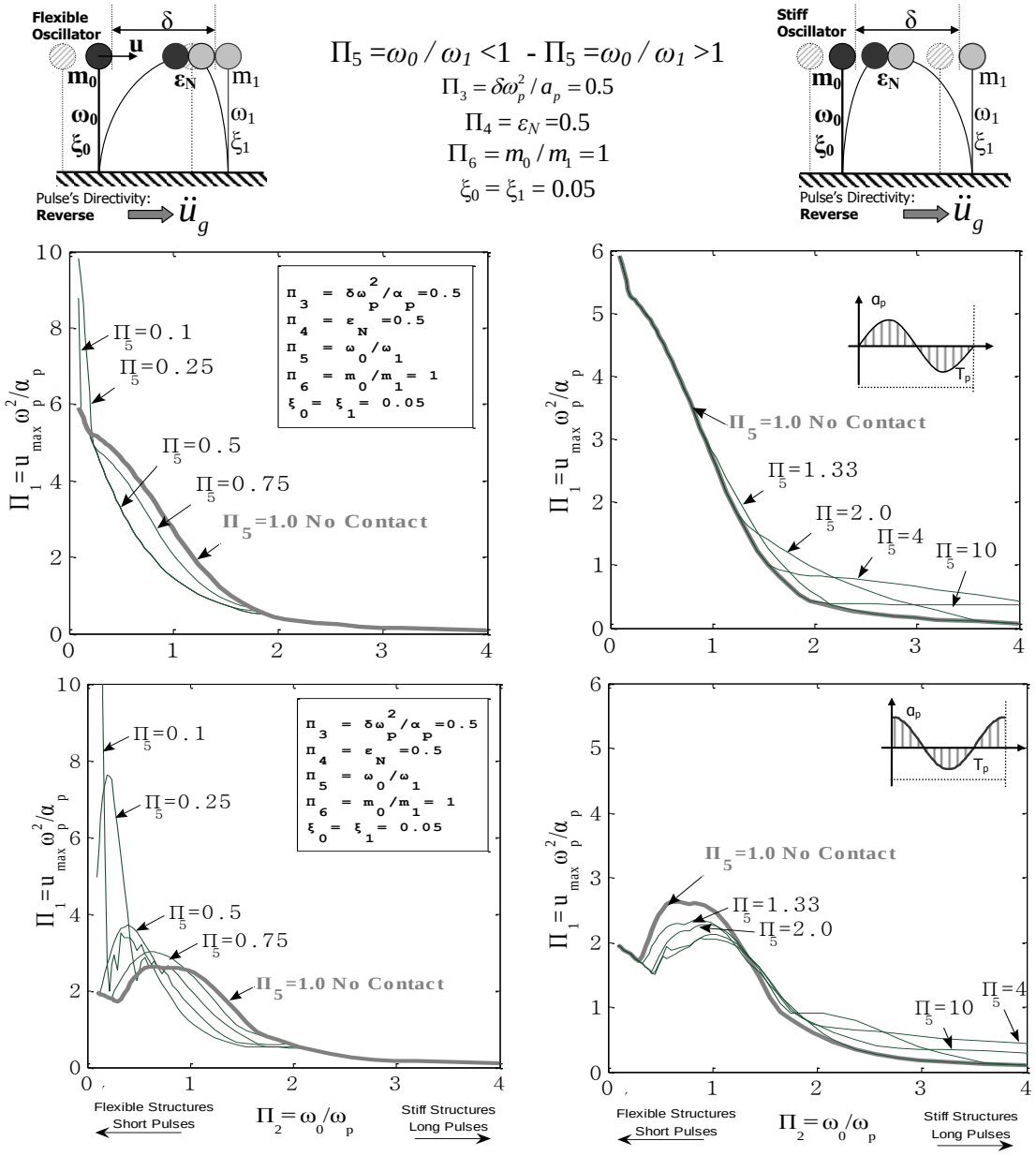

Figure 5. Self-similar response spectra (master curves) for the mechanical system of two SDOF oscillators subjected to a one sine (top) and one cosine (bottom) acceleration pulse of reverse directivity. Left column corresponds to most flexible - right column to most stiff among the two oscillators, and results are shown for several stiffness ratios

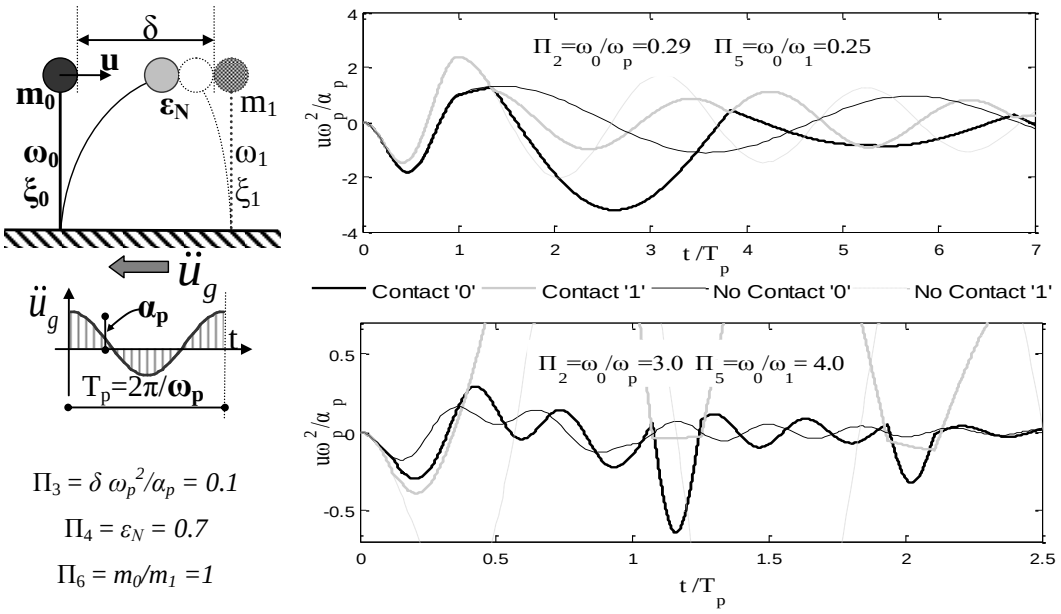

Figure 6 Amplification of the response due to contact both for the flexible (top) and the stiff (bottom) oscillator of the system

These counter-to-wide-perception conclusions, supplement what is often stated in literature, that impact amplifies the response of the stiffer oscillator and suppresses that of the more flexible (e.g. Chau & Wei [5] among others). However, when two oscillators of similar mass collide, it is their velocities that determine whether their response will amplify or deamplify, since contact is governed by impulse. Stiffness interferes only indirectly by determining frequency and thus affecting the velocity of oscillation. Accordingly, the response of a single pounding oscillator is drastically amplified in the flexible structures region, when colliding with a rigid stationary wall [17], which represents the limit case of the phenomenon, where a flexible oscillator collides with a much stiffer one.

Some of these trends are not easily observable for forward displacement (sine acceleration) pulses, but note that due to the impulsive nature of these excitations, conclusions regarding resonance are not easy to draw, even in the case of an unconstrained elastic oscillator. It is recalled that the maximum response displacement, in the dimensionless Π-products, of an unconstrained elastic oscillator excited by a sine acceleration pulse does not occur near the resonant frequency [19].

The aforementioned observations confirm that there are three distinct spectral regions, with respect to the effect of contact on the response of two SDOF pounding oscillators (Figure 7). Depending on the system's characteristics, the thresholds of each region vary, but as a general trend, there is a spectral region wherein contact amplifies the response, an intermediate region near the (original) resonance frequency, $\Pi_2 \approx 1$, wherein contact deamplifies the response of both stiff and flexible oscillators, and a third region wherein contact does not virtually affect the maximum response displacement. Similar observations about three spectral regions, referring to the same mechanical configuration, were also made by DesRoches & Muthukumar [15].

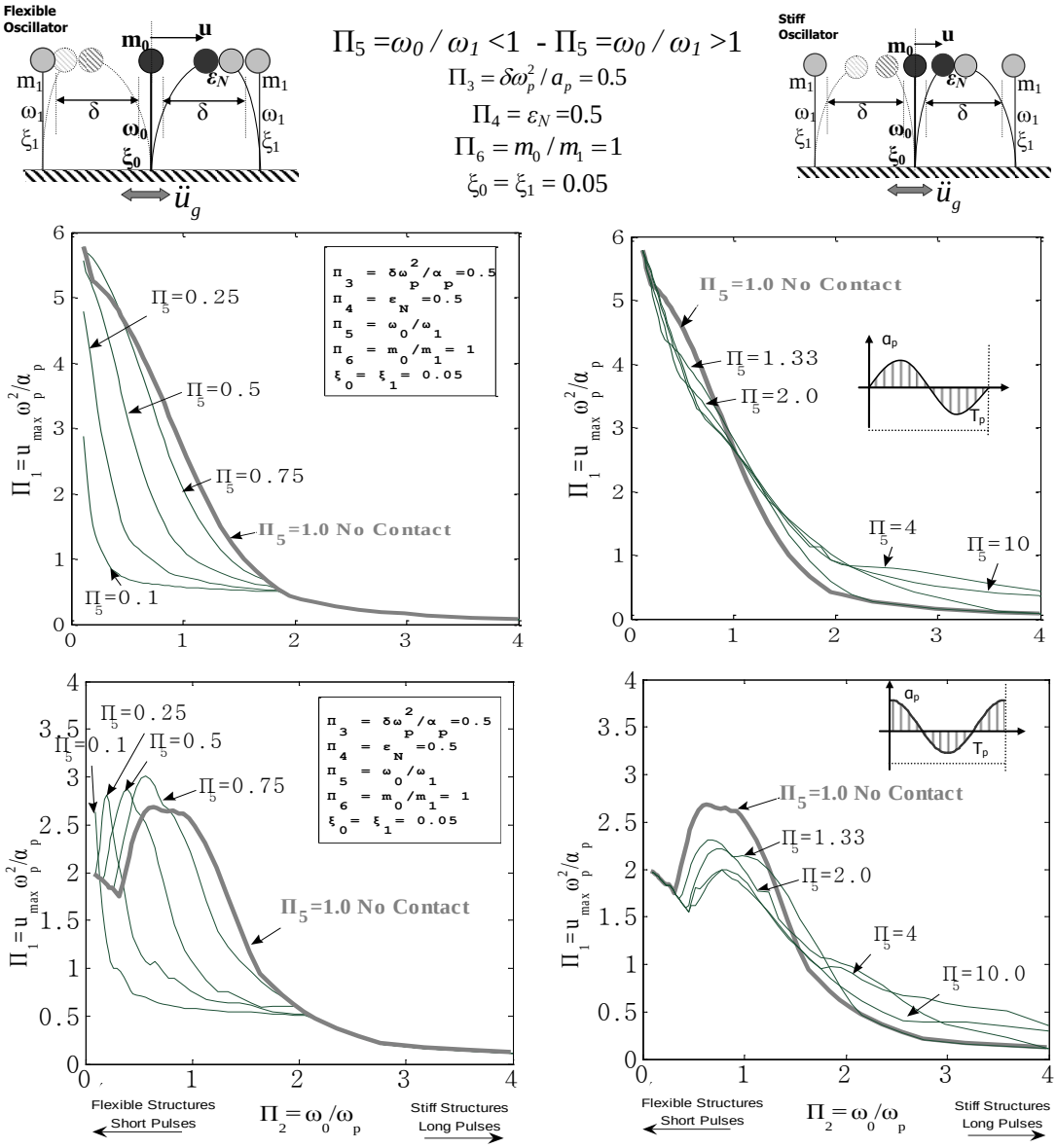

Figure 7 Self-similar response spectra (master curves) for the mechanical system of three SDOF oscillators subjected to, a one sine (top) and one cosine (bottom), acceleration pulse. Left column corresponds to most flexible - right column to most stiff among the two oscillators, and results are showted for several stiffness ratios.

Comparing with the single pounding oscillator, the difference is that the regions where contact accentuates and suppresses the response, depend on whether the oscillator is the most stiff or the most flexible of the two. In particular, the response of the most flexible oscillator is amplified in the low range of the frequency spectrum (flexible structures, small $\Pi_2=\omega_0/\omega_p = T_p/T_0$ values), whereas the response of the most stiff among the two oscillators is amplified in the upper range of the frequency spectrum (stiff structures, large $\Pi_2=\omega_0/\omega_p = T_p/T_0$ values), and vice-versa, for the spectral region wherein contact does not alter the response of stiff or flexible oscillators. Closing this section it is emphasized, that the same spectral regions are also observable for the configuration of three pounding oscillators (two-sided pounding) as Figure 7 illustrates.

COMPARISON OF ONE-SIDED AND TWO-SIDED POUNDING

In order to investigate two-sided pounding (which is a common case in bridges, as well as in buildings in series) with the simplest configuration possible, a special symmetric configuration of three SDOF oscillators in a row, where the two outer oscillators are identical and interact with the centric one which has different characteristics is considered. Comparing the response of the reference oscillator, denoted with subscript zero, of the symmetric three oscillators' pounding configuration with the asymmetric two oscillators' pounding configuration (Figure 4, Figure 5 and Figure 7), reveals the difference between single and two sided pounding.

The most notable difference in the case of two-sided pounding is the substantially smaller amplification of the maximum response displacement, particularly for flexible oscillators. This is due to the bilateral hindering of the response in case of two-sided pounding, which is more pronounced for more flexible structures. For the same reason two-sided pounding suppresses more drastically the response of stiff structures near their resonant frequency.

Another interesting trend due to pounding, is the period shift effect, towards lower frequencies, which is as pronounced for two-sided pounding as for one-sided. Consequently, the response of flexible structures may be more vulnerable for excitations with very different predominant frequencies from their unconstrained natural frequency. Or, in other words, that a short period excitation may be more crucial for a structure if pounding with an adjacent stiffer structure occurs.

THE ROLE OF m_0/m_1 RATIO

As emphasized in the Introduction, conflicting conclusions can be found with respect to the mass ratio (e.g. [15], [8], [16]) The purpose of the following discussion is to reassess the significance of mass ratio (Π_6) on the response of oscillators with unilateral contact.

Figure 8 and Figure 9 show the response spectra for constant frequency ratios, $\Pi_5 = \omega_0/\omega_1$, and dimensionless gaps, $\Pi_3 = \delta\omega_p^2/\alpha_p$, but different mass ratios, $\Pi_6 = m_0/m_1$, of the two oscillators. The main trend may be that, the smaller the mass ratio of the oscillators is, the higher the deamplification of the lighter oscillator's response (the one with the smaller mass), in agreement with Anagnostopoulos & Spiliopoulos [8]. However, very interesting counter-intuitive exceptions are also observed where the response of the lighter oscillator is deamplified. The explanation for this 'counter intuitive' behaviour, is that the velocity of the lighter oscillator is more drastically reversed by impact. As a further consequence, if this is combined with a change in sign of the ground excitation, the lighter oscillator is subsequently decelerated and hence it exhibits smaller response displacements. Similar counter intuitive responses which are also due to the accelerating and decelerating sequents of the pulses have been identified by Makris & Roussos [24] when studying the rocking response of rigid structures.

In summary, it is concluded that the mass ratio is of major importance in the response of the pounding oscillators, even when their frequencies are comparable, e.g. $\Pi_5 = \omega_0/\omega_1 = 0.75$ or 1.33 (Figure 8 and Figure 9), in agreement with the nature of contact phenomena and in particular impact, which depends on the colliding bodies' impulses. In the following section, the mechanism through which the mass ratio affects the response of pounding oscillators is further elaborated.

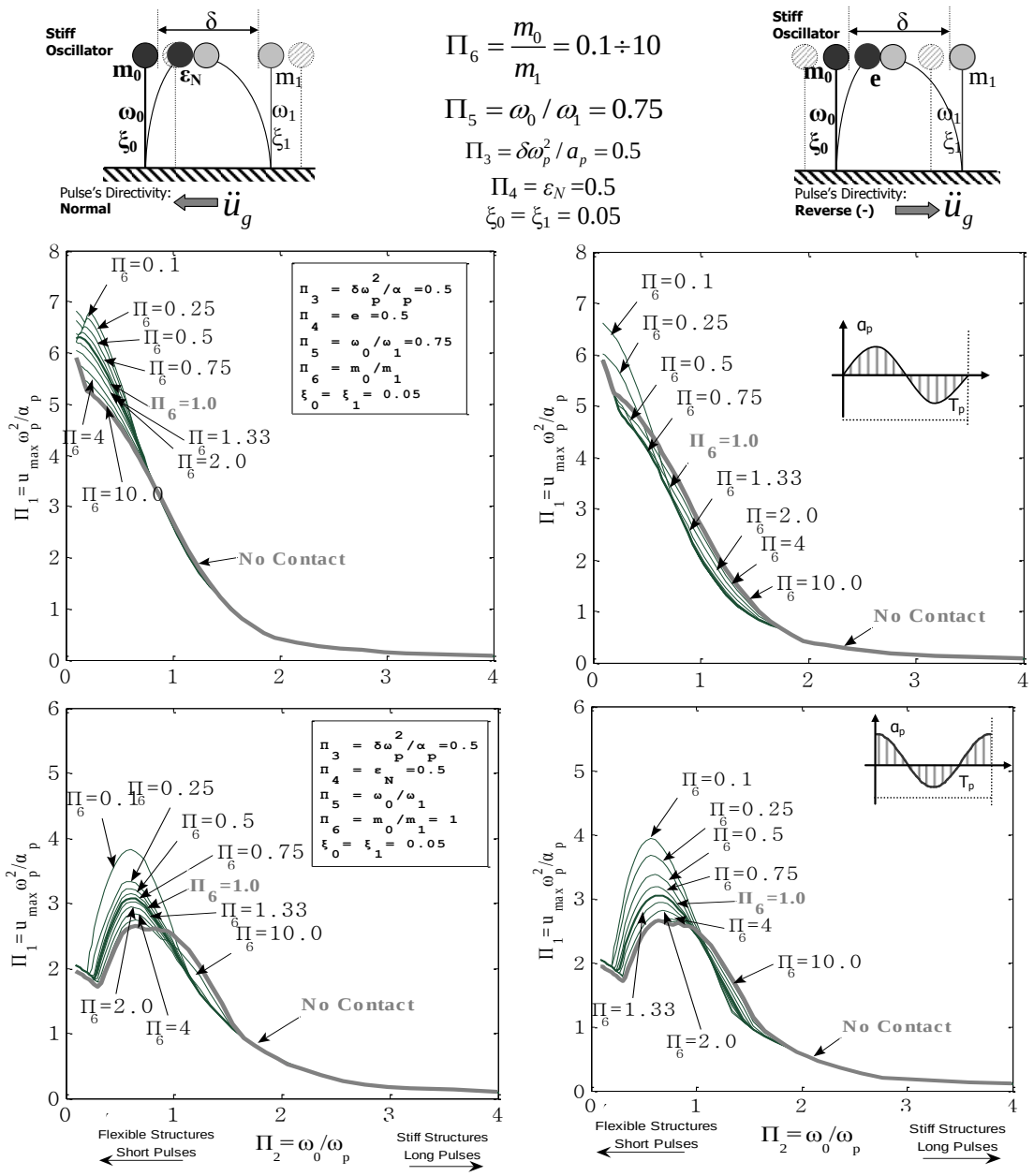

Figure 8 Self-similar response spectra (master curves) ratios of a stiff oscillator for different mass ratios. Rows correspond to different pulses and columns to different directivity.

'INTERMEDIATE ASYMPTOTICS'

In the preceding discussion the range of frequency, $\Pi_5 = \omega_0/\omega_1$, and mass ratio, $\Pi_6 = m_0/m_1$, examined ranged from 0.1 to 10, without proper justification. From a practical point of view, it is probably clear that this is the range, i.e. two orders of magnitude, of values with practical significance. However, the underlying concept with great physical significance is that of 'intermediate asymptotics' (Barenblatt, [3], [25]). In order to illustrate the mathematical representation of the notion of 'intermediate asymptotics', let there be a phenomenon of interest with two limit values of a governing parameter x, say x_1 and x_2, which differ substantially. Symbolically:

$$x_1 <<< x_2 \qquad \textbf{(11)}$$

then the asymptotic representation of specific properties of the phenomenon in the range:

$$x_1 << x << x_2 \qquad \textbf{(12)}$$

which corresponds to values large enough in comparison with the lower limit x_1, such that ($x/ x_1 \to \infty$), but at the same time small enough compared to the upper limit x_2, such that ($x/ x_2 \to 0$) is called 'intermediate asymptotics' [3], [25].

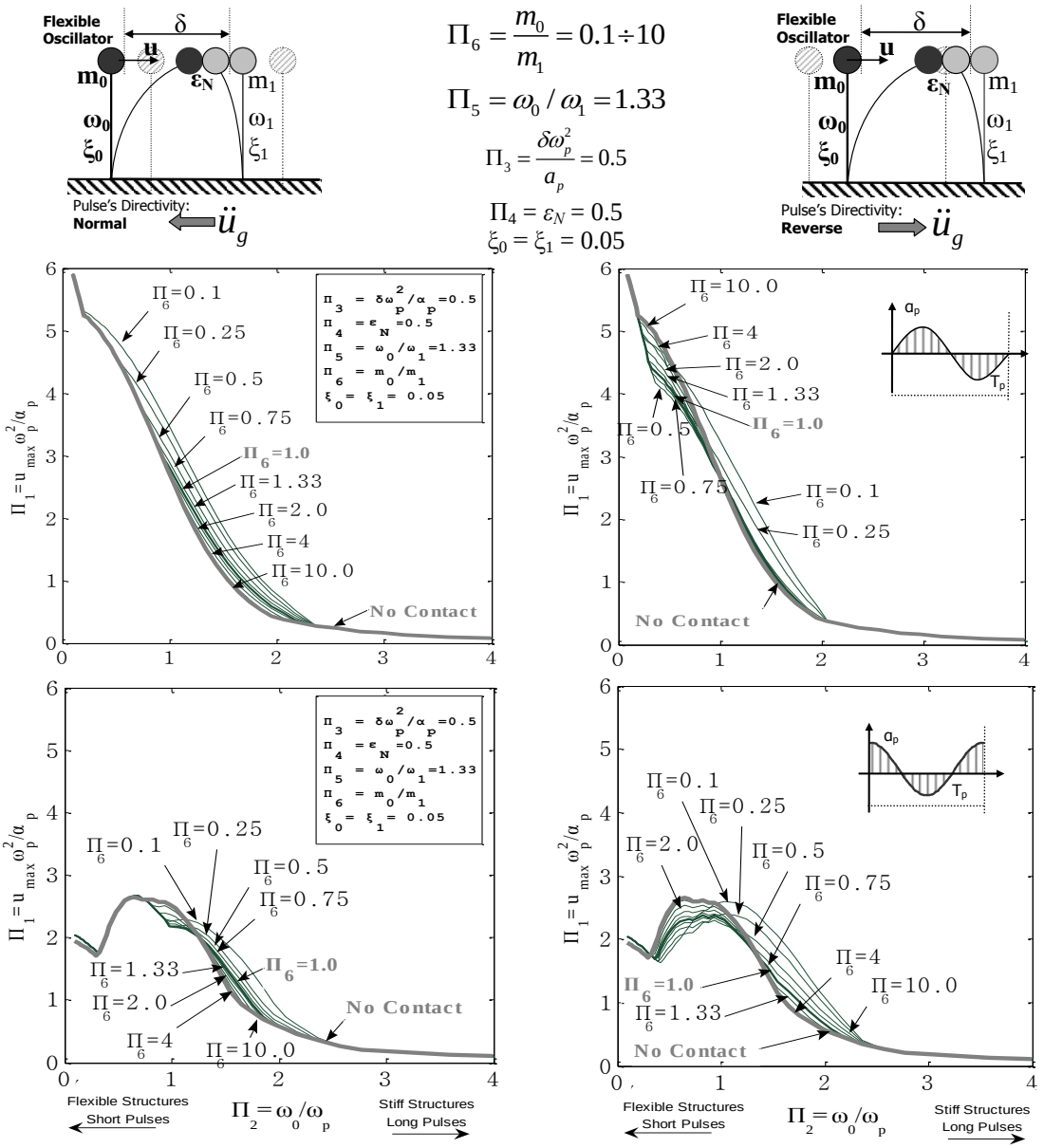

Figure 9 Self-similar response spectra (master curves) ratios of a flexible oscillator for different mass. Rows correspond to different pulses and columns to different directivity.

It is in these intermediate asymptotic states that self-similar solutions are usually encountered. Indeed, this seems the case for the problem of two SDOF pounding oscillators as well. It is in this intermediate range, from 0.1 to 10, of frequency (Π_5) and mass (Π_6) ratio, that self-similarity governs the response (Figure 10). In the limit, i.e. when Π_5 and Π_6 tend either to zero (0) or infinity (∞) the mechanical system of the two oscillators lacks physical interpretation and one must resort to other

configurations, as the SDOF pounding oscillator [17] in order to study the phenomenon.

This leads to the noteworthy remark that, the mechanical configuration of the two SDOF pounding oscillators with unilateral contact can be considered as the natural generalization of the one SDOF oscillator (Figure 2), or vice versa, that the behavior of the SDOF pounding oscillator is yielded from the limit case configuration of the two SDOF oscillators when $\Pi_5 = \Pi_6 = 0$. As a closing remark, note that the exact same reasoning holds true for the dimensionless spectral frequency, $\Pi_2 = \omega_0/\omega_p$, as well. Substantially high Π_2 values, lead to a static progress of the phenomenon, whereas for very low Π_2 values small perturbations yield unpredictable results.

INCOMPLETE SIMILARITY

Consider a physical phenomenon described by a general relationship of the form of Eq. **7.** The special case of a complete similarity or similarity of the first kind [3], [25], is when the function $\phi()$, tends to a non-zero finite limit when an independent variable Π_i becomes small (or large). This means that the function $\phi()$ is no longer sensitive to the specific variable (Π_i) and thus, this parameter, can be dropped from further consideration. However, such a limit does not always exist and hence no matter how small (or large) some variables become, they still affect the function and the associated physical phenomenon. Incomplete similarity, or similarity of the second kind, corresponds to the case where such a limit, with respect to the parameters under consideration, does not exist, yet, a scaling law does exist [3], [25], i.e. a law of the general form:

$$\Pi_1 = A\Pi_i^{\,B} \tag{13}$$

In mathematical terms this reads: the phenomenon presents the property of incomplete similarity or similarity of the second kind with respect to the dimensionless parameter Π_i under consideration.

Finding a scaling law is of major importance when considering a physical phenomenon since, in most cases scaling laws do not appear by chance, even more they offer a lucid perception of the underlying physical mechanisms. In principle, the existence of such a scaling law, of the general form of Eq. 13, can be verified in two ways [3], [25], [26]. The first is analytically, using the associated equations that describe the physical phenomenon. The second is based on the appropriate processing of the experimental or numerical results. In this particular case, following the second path, the processing of the numerical results, already presented (see Figure 8 and Figure 9), unveils the existence of a scaling law between the dependent variable Π_1 and independent variable ($\Pi_6 = m_0/m_1$), or:

$$\frac{u_{\max}\omega_p^2}{a_p} = A\left(\frac{m_0}{m_1}\right)^B \tag{14}$$

The proper processing of the results, is based on the property of scaling laws to form straight lines when showted on the logarithmic plane ($\ln\Pi_1 - \ln\Pi_6$).

$$\ln\Pi_1 = \ln A + B\ln\Pi_6 \tag{15}$$

thus, the power '*B*' becomes the slope of the straight line on the logarithmic plane and the logarithm of coefficient *A*, the point where the straight line intersects with the logarithmic scale y-y. Also note that, if the slope of the straight line is zero, then there is no dependence between the parameter under consideration (e.g. Π_1) and the governing parameter of the phenomenon (e.g. Π_6).

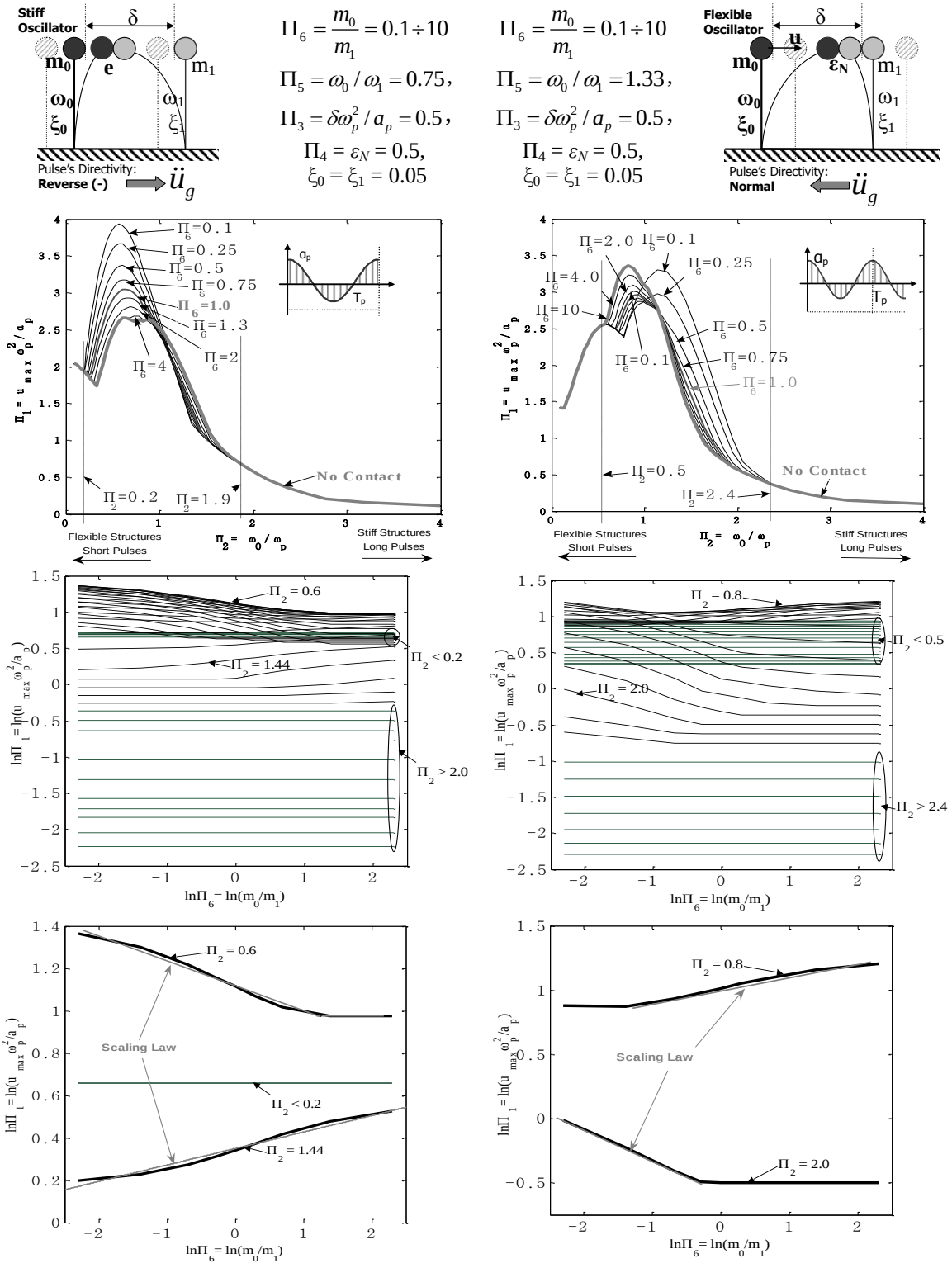

Figure 10 Top: Self-similar response spectra for different mass ratio shown in Figure 8 and Figure 9. Middle: Incomplete similarity of the response with respect to mass ratio revealed in the $\ln\Pi_1$ - $\ln\Pi_6$ plane. Bottom: the scaling laws are shown in detail.

Careful observation of Figure 8 and Figure 9 discloses the existence of three, almost straight branches on the $\ln\Pi_1$ – $\ln\Pi_6$ plane (Figure 10). From Figure 10 where

different lines correspond to distinct frequency ratios (Π_2) it is evident that, one of those three branches, is horizontal (zero slope) while the other two are of negative and positive slope, respectively. The zero slope of the first branch, according to the proceeding discussion, indicates that the maximum response displacement Π_1 is indifferent to the mass ratio Π_6, which is totally reasonable since for these spectral frequencies (Π_2 values) contact does not take place.

The other two branches, however, are practically linear and hence unveil a scaling law (Eq. 13) that correlates the maximum response displacement Π_1 with the mass ratio Π_6. The branch with negative slope corresponds to the main trend, which is that the heavier oscillator exhibits smaller response, whereas the positive inclined slope corresponds to the counter-intuitive behavior, both described in a previous section. In mathematical terms this reads: the response presents the property of incomplete similarity with respect to mass ratio (dimensionless Π_6 –product). The applicability of this scaling law should be further investigated in order to derive, if feasible, a closed-form expression for equation (14)**.**

CONCLUSIONS

The aim of the present paper is to elucidate the earthquake response of pounding oscillators, a subject characterized by large number of parameters for which conflicting conclusions have been presented in the past. The present study revisits the problem by using formal dimensional analysis in an effort to identify distinct physical similarities.

The application of the proposed method hinges upon the existence of a distinct time and length scale that characterizes the most energetic component of ground shaking. It condenses the parametric analysis, since the number of dimensionless Π-products that govern the response are three (3) less than the number of independent variables. Furthermore, it unveils the remarkable symmetry of self-similarity and the existence of a scaling law, hidden into the response. In particular, when the response is presented in terms of the dimensionless Π-products, response curves for any excitation level collapse to a single master curve, whereas response curves for different mass ratios and distinct frequency ratios follow, within an intermediate asymptotic state, a scaling law; the latter in mathematical terms is known as incomplete similarity.

The present analysis also concludes that due to pounding, the response of the most flexible, among a pair of two oscillators, is amplified in the low range of the frequency spectrum; while the response of the most stiff oscillator is amplified in the upper range of the frequency spectrum. The existence of three distinct spectral regions with respect to the effect of pounding on elastic oscillators is confirmed both for the two and three pounding oscillators' configuration. The practical significance of these observations is that real-life structures, such as colliding buildings or interacting bridge segments, may be most vulnerable for excitations with frequencies very different from their natural eigenfrequencies.

Finally, the comparison of one-sided and two-sided pounding revealed that the amplification of the response in the case of two-sided pounding is substantially limited, yet, the period shift effect of pounding is as prominent as in the one-sided pounding, thus drastically altering the dynamic behavior of the mechanical configuration.

ACKNOWLEDGMENTS

Partial financial support to the first author was provided by the Marie Curie fellowship (HPMT-GH-01-00359-16).

REFERENCES

1. Langhaar HL. *Dimensional Methods and Theory of Models.* London: John Wiley & Sons: 1951
2. Sedov LI. *Similarity and Dimensional Methods of Mechanics*. Academic Press: New York, 1959
3. Barenblatt GI. *Scaling, Self-Similarity, and Intermediate Asymptotics*. Cambridge Univ. Press: Cambridge, UK, 1996
4. Davis RO. Pounding of buildings modeled by an impact oscillator. *Earthquake Engng. Struct. Dyn*., 1992; **21**:253-274
5. Chau KT, Wei XX. Pounding of structures modelled as non-linear impacts of two oscillators. *Earthquake Engng Struct. Dyn*. 2001; **30**:633-651
6. Anagnostopoulos S A. Pounding of buildings in series during earthquakes. *Earthquake Engng. Struct. Dyn*. 1988; **16**: 443-456
7. Anagnostopoulos S A. Earthquake induced pounding: State of the art. *10th European Conference on Earthquake Engineering*. Duma (ed.) 1995 Balkena, Rotterdam
8. Anagnostopoulos S A, Spiliopoulos K V. An investigation of earthquake induced pounding between adjacent buildings. *Earthquake Engng. Struct. Dyn*. 1992; **21**: 289-302
9. Penelis GG, Kappos AJ. *Earthquake-resistant concrete structures*. E & FN SPON (Chapman & Hall): London, 1997
10. Maragakis E, Jennings PC, Analytical Models for the Rigid Body Motions of Skew Bridges. *Earth. Eng. And Str. Dyn*. 1987; **15:** 923-944
11. Liolios AA. A Linear Complementarity Approach to Non-Convex Dynamic Problem of Unilateral Contact with Friction between Adjacent Structures. ZAMM (*Journal of Applied Mathematics and Mechanics)*, 1989; **69**(5):420-422.
12. Panagiotopoulos PD. Dynamic and Incremental Variational Inequality Principles, Differential Inclusions and Their Applications to Co-Existent Phases Problems. *Acta Mechanica*, 1981; **40**:85–107
13. Athanassiadou CJ, Penelis GG, Kappos AJ. Seismic response of adjacent buildings with similar or different dynamic characteristics. *Earthquake Spectra*, 1994; **10**(2): 293–317.
14. Jankowski R, Wilde K, Fujino Y. Pounding of Superstructure Segments in Isolated Elevated Bridge During Earthquakes. *Earthquake Engng. Struct. Dyn*. 1998; **27**: 487-502
15. DesRoches R, Muthukumar S. Effect of Pounding and Restrainers on Seismic Response of Multiple-Frame Bridges. *Journal of Structural Engineering* (ASCE) 2002, **128**(7): 860-869
16. Ruangrassamee A, Kawashima K. Relative displacement response spectra with pounding effect. *Earthquake Engng Struct. Dyn*. 2001; **30**:1511–1538
17. Dimitrakopoulos EG, Makris N, Kappos AJ. Dimensional Analysis of Pounding Oscillators. *6th GRACM International Congress on Computational Mechanics*, Thessaloniki, 19-21 June 2008 (accepted for publication)
18. Makris N, Black CJ. Dimensional Analysis of Rigid-Plastic and Elastoplastic Structures under Pulse-Type Excitations *Journal of Engineering Mechanics* (ASCE) 2004; **130** (9) 1006-1018

19. Makris N, Black CJ. Dimensional Analysis of Bilinear Oscillators under Pulse-Type Excitations *Journal of Engineering Mechanics* (ASCE) 2004; **130** (9):1019-1031
20. Makris N, Black CJ. Evaluation of Peak Ground Velocity as a ‘‘Good’’ Intensity Measure for Near-Source Ground Motions. *Journal of Engineering Mechanics* (ASCE) 2004; **130(**9): 1032-1044
21. Makris N, Psychogios C. Dimensional Response Analysis of Yielding Structures with first-Mode Dominated Response. *Earthquake Engng Struct. Dyn*. 2006; **35**:1203–1224
22. Pfeiffer F, Glocker C. *Multibody Dynamics with Unilateral Contacts.* Wiley: New York, 1996
23. Leine RI., van Campen DH, Glocker C. Nonlinear Dynamics and Modeling of Various Wooden Toys with Impact and Friction. *Journal of Vibration and Control*, 2003; **9**: 25-78
24. Makris N, Roussos Y. Rocking response of rigid blocks under near-source ground motions. *Geotechnique*, 2000, **50**(3): 243–262
25. Barenblatt GI. *Scaling*. Cambridge Univ. Press: Cambridge, U.K., 2003
26. Barenblatt GI. Scaling phenomena in fatigue and fracture. *International Journal of Fracture*, 2006; **138**:19–35